

## UV meteor observation from a space platform

P. SCARSI(\*)

*INAF, Istituto di Astrofisica Spaziale e Fisica Cosmica, sez. Palermo - Palermo, Italy  
AREA CNR - Via U. La Malfa 153, 90146 Palermo, Italy*

*(Nuovo Cimento C, 27 (2004) 359-381)*  
DOI 10.1393/ncc/i2004-10033-y

With reference to *Il Nuovo Cimento C*, Vol. **27**, N. 4, Luglio-Agosto 2004, pp. 359-381, because of a trivial numerical error in the input value assumed for the “Heat of ablation”, some of the tables and figures in the paper reporting the results from a set of computations obtained in runs of the meteor code developed have been revised. The corrections concern table I, figures from 4 to 9 and the text of sect. **7**: “Meteor dependence on parametric values” (p. 374 and following).

### 7. – Meteor dependence on parametric values

The range of mass values to which the “ablation regime” can be applied is limited on the low mass side ( $10^{-8}$ – $10^{-9}$ ) kg by the competing process of heat transfer to the interior of the meteoroid giving rise to an increase in the global temperature of the solid body reaching the melting point, with a transition to the “micrometeorite regime” with no ablation and the cooling assured by Planck radiation and the other processes of transfer to the surrounding medium (see sect. **8**).

Table I gives, as a function of the initial mass of the meteoroid, the Magnitudo corresponding to  $UV_{Max}$ , the  $UV_{Max}$  altitude, altitude of start and end of detectable UV emission above a given threshold value, track length and duration above threshold.

Figure 4 gives, at various values of threshold for the UV-Magnitudo, the start and end altitude for the observable meteor as a function of the initial mass value.

As a function of Magnitudo threshold: at  $M_{UV-Threshold} = 18$  for  $m_0 = 10^{-8}$  kg the observable track length is still 120 km; at  $M_{UV-Threshold} = 0$  meteors are observable down to  $m_0 \sim 10^{-3}$  kg; for  $m_0 > 10^{-1}$  kg meteors tracks are observable at  $M_{UV-Threshold} = -6$  (“naked eye” equivalent in the optical band).

Figure 5 gives the duration of the observation *vs.* the initial mass value parameterized for the Magnitudo at threshold value  $M_{UV-Threshold} = 18, 12, 6, 0, -6$ .

---

(\*) E-mail: paolo.scarsi@pa.iasf.cnr.it

TABLE I. – Ablation only ( $v_0 = 35$  km/s,  $\theta = 35^\circ$ ).

Mass (kg)	UV <sub>Max</sub> ( $M_{UV}$ )	Altitude-UV <sub>Max</sub> (km)	Altitude-Start (km)	Altitude-End (km)	Track Length (km)	Duration (s)
Threshold = 18 ( $M_{UV}$ )						
1	-9.41	6.93	483.05	0.05	833.40	23.84
$10^{-1}$	-6.91	12.27	392.62	0.02	676.88	19.66
$10^{-2}$	-4.41	17.60	311.15	0.00	536.07	16.92
$10^{-3}$	-1.91	23.03	241.77	1.68	413.28	15.00
$10^{-4}$	0.59	28.36	185.85	7.91	306.21	12.00
$10^{-5}$	3.09	33.79	148.36	14.22	230.81	9.87
$10^{-6}$	5.59	39.12	126.08	20.64	181.04	7.40
$10^{-7}$	8.09	44.54	113.19	27.26	147.86	5.70
$10^{-8}$	10.60	49.88	104.39	34.15	120.87	4.41
$10^{-9}$	18.08	56.26	-	-	-	-
Threshold = 12 ( $M_{UV}$ )						
1	-9.41	6.93	206.98	0.05	356.34	10.27
$10^{-1}$	-6.91	12.27	161.74	0.02	278.36	8.33
$10^{-2}$	-4.41	17.60	133.33	0.00	229.39	8.21
$10^{-3}$	-1.91	23.03	117.69	3.87	195.78	8.00
$10^{-4}$	0.59	28.36	107.46	10.36	167.03	6.66
$10^{-5}$	3.09	33.79	97.95	17.07	139.13	5.22
$10^{-6}$	5.59	39.12	87.20	24.14	108.51	3.89
$10^{-7}$	8.09	44.54	76.36	31.83	76.65	2.65
$10^{-8}$	10.60	49.88	65.00	41.22	41.00	1.37
Threshold = 6 ( $M_{UV}$ )						
1	-9.41	6.93	111.14	0.05	191.22	5.58
$10^{-1}$	-6.91	12.27	102.24	0.02	175.89	5.42
$10^{-2}$	-4.41	17.60	91.50	0.00	157.17	5.00
$10^{-3}$	-1.91	23.03	80.75	6.95	126.96	4.67
$10^{-4}$	0.59	28.36	70.01	14.23	95.96	3.38
$10^{-5}$	3.09	33.79	59.08	22.38	63.18	2.15
$10^{-6}$	5.59	39.12	46.01	34.00	20.79	0.69
Threshold = 0 ( $M_{UV}$ )						
1	-9.41	6.93	74.31	0.05	127.82	3.78
$10^{-1}$	-6.91	12.27	63.56	0.02	109.31	3.53
$10^{-2}$	-4.41	17.60	52.81	4.43	83.23	2.89
$10^{-3}$	-1.91	23.03	41.60	13.28	48.78	1.64
Threshold = -6 ( $M_{UV}$ )						
1	-9.41	6.93	35.50	0.05	61.07	1.89
$10^{-1}$	-6.91	12.27	23.60	5.07	31.96	1.06

Decimal digits derive strictly from computation and therefore they do not have necessarily “physical” relevance.

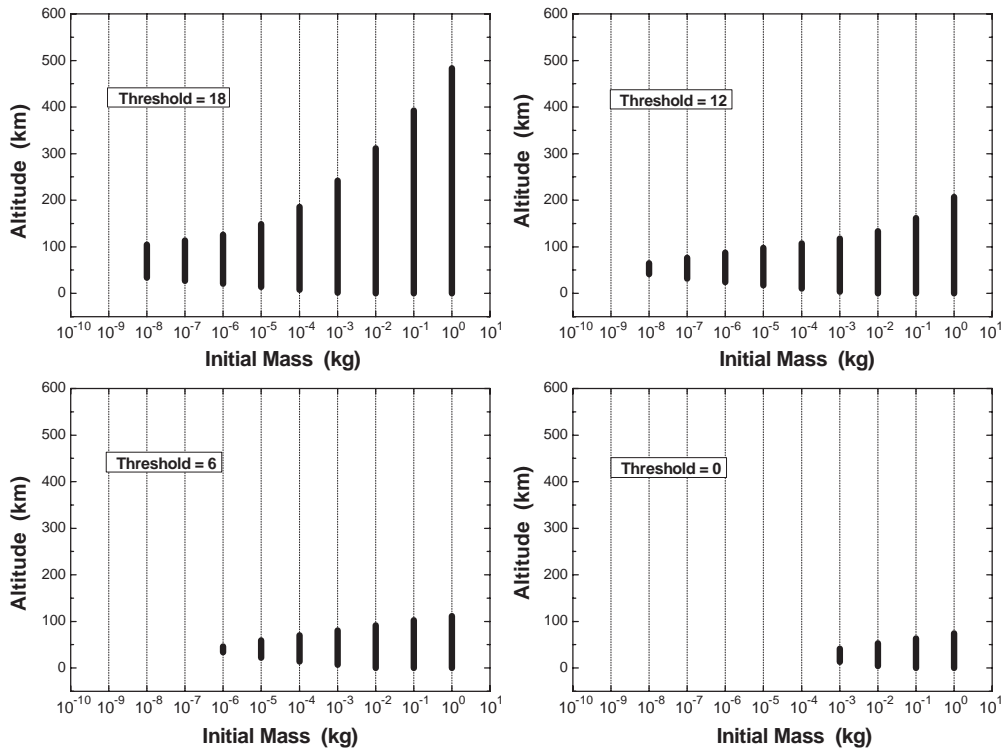


Fig. 4. – Start and end altitude for the observable meteor track as a function of the initial mass value at various values of threshold for the UV-Magnitude (“pure ablation process”; entry at 900 km with  $v_0 = 35$  km/s and  $\theta = 35^\circ$ ).

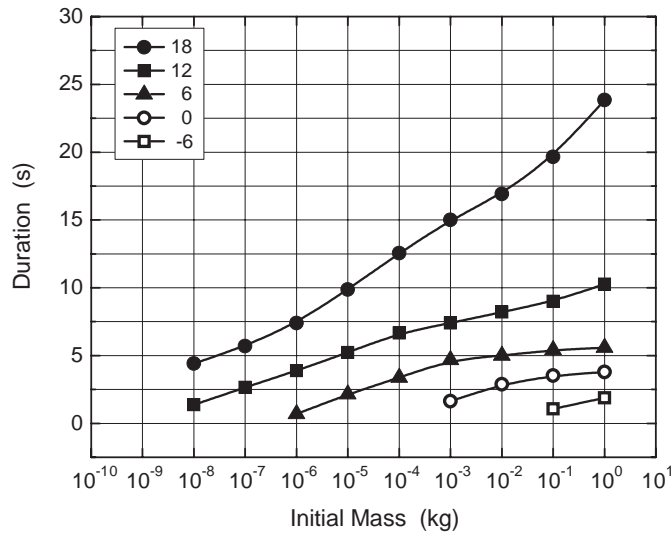


Fig. 5. – Duration of observation *vs.* the initial mass value parameterized for the Magnitudo at threshold value  $M_{\text{Threshold}} = 18, 12, 6, 0, -6$  (“pure ablation process”; entry at 900 km with  $v_0 = 35$  km/s and  $\theta = 35^\circ$ ).

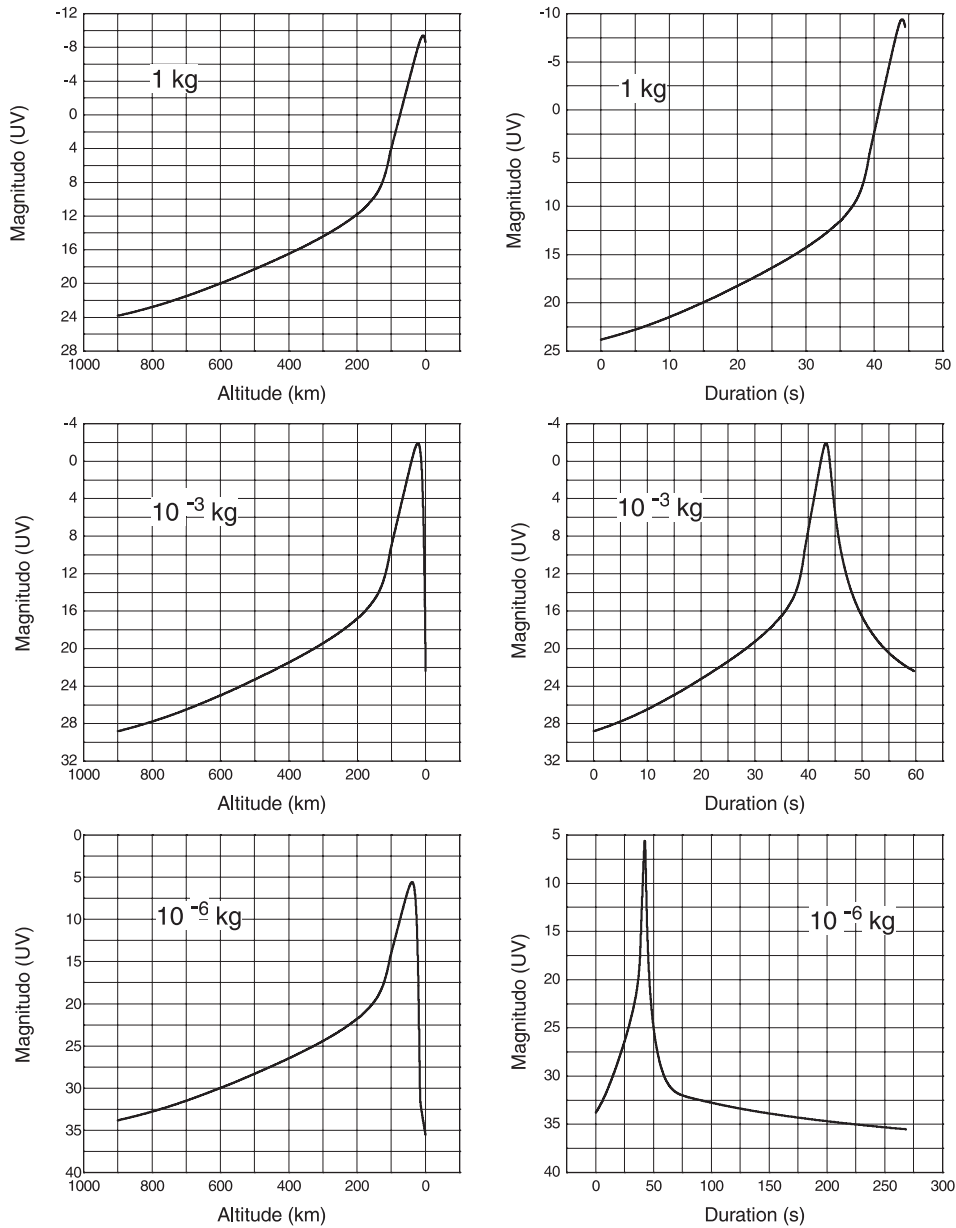


Fig. 6. – Ablation process only:  $v_0 = 35$  km/s and  $\theta = 35^\circ$ . UV-Magnitude *vs.* altitude a.s.l. and *vs.* duration for different values of the initial mass.

Figure 6 shows, as examples, results obtained for the UV-Magnitude track profile *vs.* altitude a.s.l. and *vs.* meteor duration for some initial mass values and  $v_0 = 35$  km/s and  $\theta = 35^\circ$ . The simulations show that the meteor phenomenon is on-setting high in the atmosphere reaching a value of  $M_{UV} \sim 18$  at  $h \sim 500$  km for  $m_0 = 1$  kg and at  $h \sim 250$  km for  $m_0 = 10^{-3}$  kg. As the process goes on, the luminosity keeps increasing with depth

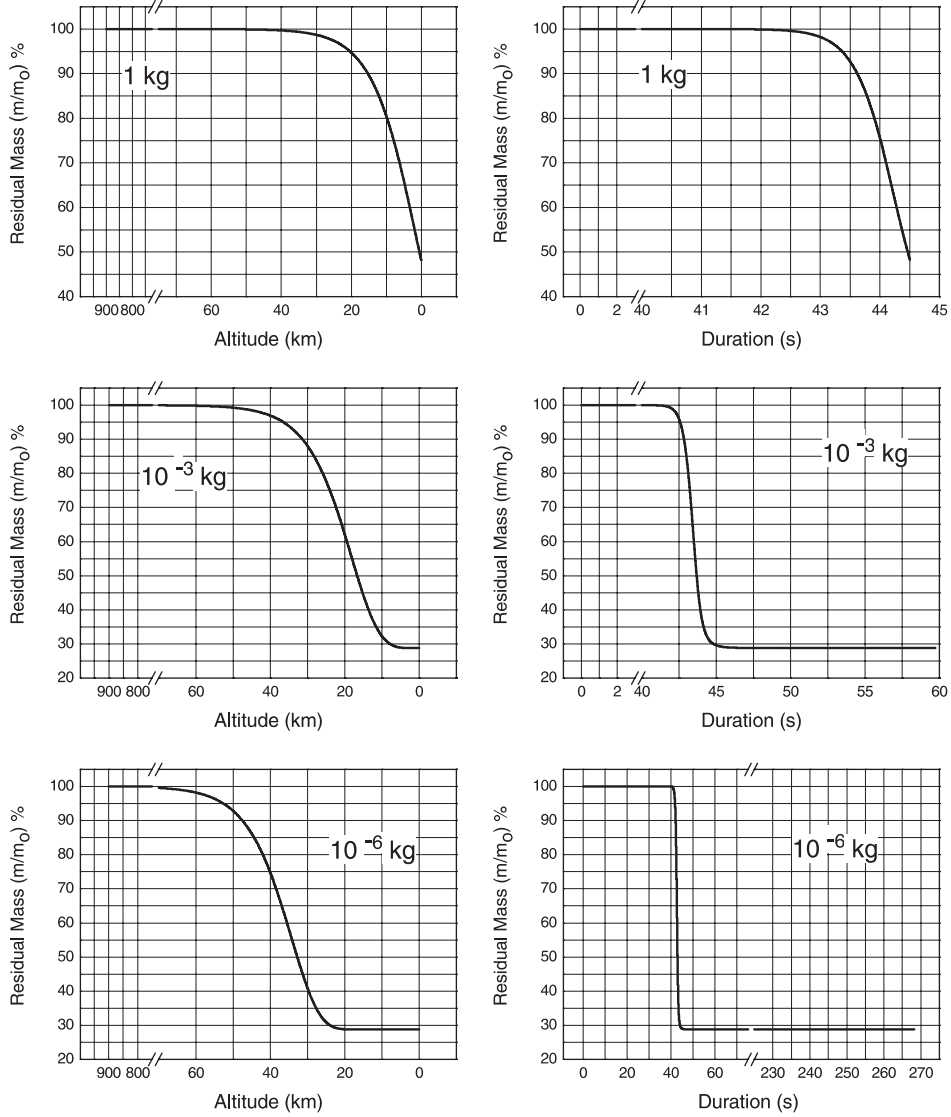


Fig. 7. – Ablation process only:  $v_0 = 35$  km/s and  $\theta = 35^\circ$ . Residual mass *vs.* altitude a.s.l. and *vs.* duration for different values of the initial mass.

of penetration, reaching a maximum of luminosity  $M_{UV-Max} \sim (-9)$  at  $h \sim 7$  km; the corresponding value for an initial mass  $m_0 = 10^{-3}$  kg is  $M_{UV-Max} \sim (-2)$  at  $h \sim 23$  km and  $M_{UV-Max} \sim 6$  at  $h \sim 39$  km for initial mass  $m_0 = 10^{-6}$  kg.

The fall in luminosity is abrupt after maximum.

The rate of mass ablation is evaluated in fig. 7. It starts to be appreciable at  $\sim 30$  km for  $m_0 = 1$  kg with a residual mass value at ground (meteorite)  $m \sim 0.48$  kg; for  $m_0 = 10^{-3}$  kg, the corresponding values are:  $h \sim 43$  km with a meteorite mass  $m \sim 2.9 \times 10^{-4}$  kg and for  $m_0 = 10^{-6}$  kg,  $h \sim 60$  km with a meteorite mass  $m \sim 2.9 \times 10^{-7}$  kg. For the set of initial conditions assumed in the simulations, for  $m_0 > 10^{-9}$  kg the process

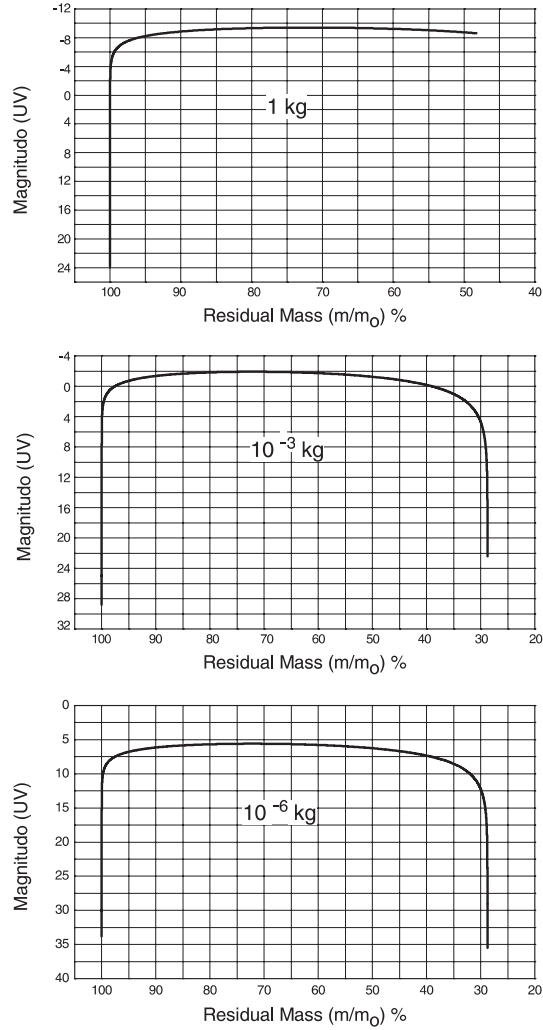


Fig. 8. – Ablation process only:  $v_0 = 35$  km/s and  $\theta = 35^\circ$ . UV-Magnitude *vs.* residual mass for different values of the initial mass.

always ends with a residual meteorite with an asymptotic  $m/m_0 \sim 0.29$  reached below  $m_0 \sim 10^{-2}$  kg.

Figure 8 shows the UV-Magnitude *vs.* the ratio residual/initial mass in the ablation process for initial mass values 1 kg,  $10^{-3}$  kg and  $10^{-6}$  kg. The UV-Magnitude rises abruptly to  $M_{UV-Max}$  for the first few percents of mass loss and drops sharply near the end of the ablation process.

In the different run sets described above, the initial values for the meteoroid mass are parameterized while velocity and angle of entry and all the other quantities ( $C_D$ ,  $\zeta$ ,  $\Delta$ ,  $\tau$ ,  $C.I.$  ...) are kept unchanged.

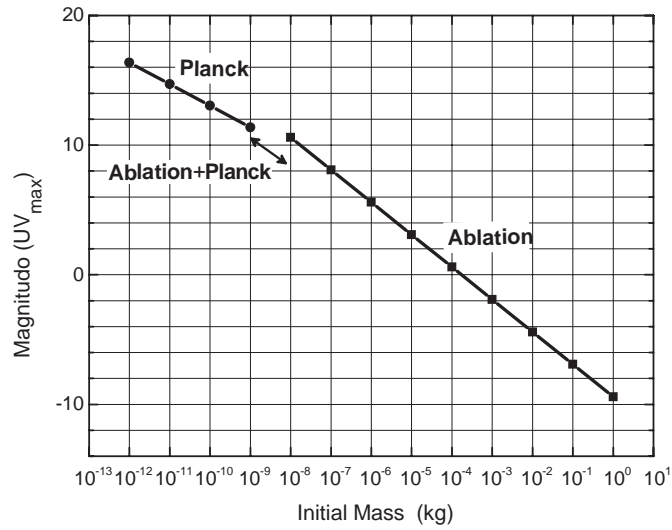


Fig. 9. – Value of the maximum value reached by the meteor UV-Magnitude as a function of the initial mass of the meteoroid and fixed entry values:  $v_0 = 35$  km/s,  $\theta = 35^\circ$ ; only Planck emission from the heating process is considered for  $m < 10^{-9}$  kg and only the ablation process is considered above the  $10^{-8}$  kg limit.

Figure 9 shows with black filled squares for the pure ablation process (entry at 900 km with  $v_0 = 35$  km/s and  $\theta = 35^\circ$ ) the maximum value reached by the meteor luminosity, expressed in UV-Magnitude, as a function of the initial mass in the range  $10^{-8}$  kg to 1 kg.